

Expanding the cultivated human archaeome by targeted isolation of novel *Methanobrevibacter* strains from fecal samples

Stefanie Duller¹, Simone Vrbancic¹, Łukasz Szydłowski^{2,3}, Alexander Mahnert^{1,4}, Marcus Blohs¹, Michael Predl^{5,6}, Christina Kumpitsch^{1,2}, Verena Zrim⁷, Christoph Högenauer⁸, Tomasz Kosciolek^{2,3,9}, Ruth A. Schmitz¹⁰, Anna Eberhard¹, Melanie Dragovan¹, Laura Schmidberger¹, Tamara Zurabischvili¹, Viktoria Weinberger¹, Adrian Mathias Moser⁸, Dagmar Kolb¹¹, Dominique Pernitsch¹¹, Rokhsareh Mohammadzadeh¹, Torben Kühnast¹, Thomas Rattei⁵, Christine Moissl-Eichinger^{1,4*}

¹ D&R Institute of Hygiene, Microbiology and Environmental Medicine, Medical University of Graz, Graz, Austria;

² Malopolska Centre of Biotechnology, Jagiellonian University in Krakow, Poland;

³ Sano Centre for Computational Medicine, Krakow, Poland

⁴ BioTechMed Graz, Graz, Austria;

⁵ Centre for Microbiology and Environmental Systems Science, University of Vienna, Vienna, Austria;

⁶ Doctoral School Microbiology and Environmental Science, University of Vienna, Vienna, Austria

⁷ Center for Medical Research, Medical University of Graz, Graz, Austria;

⁸ Division of Gastroenterology and Hepatology, Department of Internal Medicine, Medical University of Graz, Graz, Austria;

⁹ Department of Data Science and Engineering, Silesian University of Technology, Gliwice, Poland;

¹⁰ Institute for General Microbiology, Christian Albrechts University, Kiel, Germany;

¹¹ Core Facility Ultrastructure Analysis, Medical University of Graz, Graz, Austria;

*Corresponding author

christine.moissl-eichinger@medunigraz.at

Abstract (250 words)

Archaea are integral components of the human microbiome but persist as understudied entities within the gastrointestinal tract (GIT), primarily due to the lack of cultured representatives for comprehensive mechanistic investigations. With only four *Methanobrevibacter smithii* isolates from humans available according to the Global Catalogue of Microorganisms (GCM), the existing cultures fail to adequately represent the observed diversity, as underscored by recent findings.

This study introduces a targeted cultivation method for enriching methanogenic archaea from human fecal samples. Applied to 16 stool samples from healthy and diseased donors, the method aimed to genomically characterize the archaeal cultures and establish correlations with gastrointestinal disorders. The procedure combines methane breath testing, *in silico* metabolic modelling, media optimization, FACS, dilution series, and genomic sequencing through Nanopore technology. Additional analyses include co-cultured bacteriome, comparative genomics of archaeal genomes, functional comparisons, and structure-based protein function prediction of unknown differential traits.

Successful establishment of stable archaeal cultures from 14 out of 16 fecal samples yielded nine previously uncultivated strains, eight of which were absent from a recent archaeome genome catalog. Comparative genomic and functional assessments of *Methanobrevibacter smithii* and *Candidatus Methanobrevibacter intestini* strains from diverse participant cohorts revealed features potentially associated with gastrointestinal diseases.

This work substantially broadens the scope of available archaeal representatives for functional and mechanistic studies in the human GIT. The established protocol facilitates the cultivation of methanogenic archaea from nearly every human fecal sample, offering insights into the adaptability of *Candidatus Methanobrevibacter intestini* genomes in critical microbiome situations.

Introduction

The human gut is a complex ecosystem harboring a diverse community of microbes, including bacteria, fungi, viruses, and archaea (1). While bacteria are well described, and their role in gut health is well studied, the function and role of archaea in the human gastrointestinal tract (GIT) is still not well understood. Archaea found in the GIT are mainly represented by the order Methanobacteriales, with the most abundant species *Methanobrevibacter smithii* and *Candidatus Methanobrevibacter intestini* (2–4).

These methanogenic archaea produce methane (CH₄) as a metabolic byproduct, while producing ATP via methanogenesis (5–9). The yielded CH₄ serves as an important indicator for the presence of methanogenic archaea (10).

CH₄ can be detected in humans' breath, as it is partially absorbed into the blood and excreted through the lungs (11). The impact of CH₄ on the human GIT has already been addressed and it has been reported that CH₄ leads to the reduced efficiency of intestinal smooth muscle activity, often associated with e.g. the constipation-predominant irritable bowel syndrome (12–14). Further, variations of CH₄ levels in the human breath were discussed as an indicator for enhanced oxidative stress and could therefore show a great potential for example in *in vivo* diagnostics (15–17). On the other hand, positive effects were also described, as CH₄ could also act as antioxidant, protecting cells from reactive oxygen species (ROS) and demonstrating potential anti-inflammatory properties (18).

Methanobrevibacter species show a prevalence of more than 90% in fecal samples with an average abundance of 0.56 % for *Methanobrevibacter smithii* and 0.13 % for *Cand. Methanobrevibacter intestini* (3,19). In high-CH₄ producing individuals (up to 40% of the middle European and Northern American population) (20), this average abundance is raised to 2 % for *Methanobrevibacter* genus in general (21).

Notably, *Methanobrevibacter* species are highly correlated with certain bacterial representatives of the gut microbiome, e.g. Christensenellaceae, and have been shown to be syntrophically interactive in co-culture experiments with e.g. *Christensenella minuta* or *Bacteroides thetaiotaomicron* (22,23).

Even though (methanogenic) archaea have been shown to be part of the human gut microbiome for more than 40 years (24), knowledge about their function and role within the human gut microbiome is still sparse. The reason for this lies in several

methodological issues as standard protocols are mainly bacteria-optimized, which are not optimally working for archaea due to their distinct cell structure, physiology, and metabolic activity. These distinct features and inappropriate protocols make it difficult to visualize, culture or analyze them with multi-omics approaches (25).

Furthermore, the lack of comprehensive reference databases poses a challenge in adequately evaluating methanogenic archaea in the datasets. Additionally, the presence of a strong bacterial or host background further complicates the matter (25). Therefore, it is of utmost importance to develop new protocols or modify existing ones to effectively study archaea in the complex microbiome environment.

Even though molecular biological techniques help to study the archaeome, isolating and culturing archaea is crucial for in-depth, mechanistic analysis of these microbes. Based on the Global Catalogue of Microorganisms (<https://gcm.wdcm.org/>) only few human host-associated archaeal isolates are available in culture (three *Methanobrevibacter oralis* strains from human oral cavity and subgingival plaque; and four *Methanobrevibacter smithii* isolated from human feces and large intestine), hindering detailed studies.

To tackle the lack of archaeal cultures for functional studies, we established herein a culturing procedure to efficiently enrich and isolate methanogenic archaea from human stool samples in a targeted manner. By providing optimal growth conditions (e.g. by providing a suitable bacterial partner), followed by archaea-targeting Fluorescence-Activated Cell Sorting (FACS), dilution series and quality control through Nanopore sequencing, we were able to establish stable methanarchaeal cultures—from 14 out of 16 fecal samples obtained from both healthy and diseased subjects.

By this procedure, we obtained 9 novel methanarchaeal strains, and were able to retrieve personalized representatives of *Methanobrevibacter smithii* and *Cand. Methanobrevibacter intestini* strains from stool samples of various participants with different health conditions, which were subsequently compared on genomic and functional levels.

As the role of archaea in health and disease is still unknown and it is still discussed whether they might have a potential beneficial or a pathogenic effect on human health, obtaining additional isolates from human samples will allow in-depth analysis, which might help to deepen our understanding of the role of methanogens in the human GIT.

Material and Methods

Ethics and participant recruitment

Sixteen participants with different health conditions (healthy or with any kind of gastrointestinal disorder) were recruited based on their baseline breath CH₄ levels (> 5 ppm / high CH₄ emitters). The recruitment was supported by medical doctors at the State Hospital Graz (Austria) and an independent physician also located in Graz, Austria. Participants were asked to undergo a breath test, provide a stool sample, and complete a questionnaire with health status information (Supplementary Table S1). Further, all participants signed an informed consent before participation. A list of exclusion and inclusion criteria can be found in Supplementary Table S2. The study was approved by the local ethics committee at the Medical University of Graz, Austria (EK-Nr: 31-452 ex 18/19).

Sample collection, processing and storage

For the pre-selection of participants, a breath test was performed as previously described (21). For this purpose, participants performed the breath test either directly on a GastroCH₄ECKTM Gastrolyzer (Bedfont Scientific Ltd., UK) or with a GastroCH₄ECKTM breath bag (Bedfont Scientific Ltd., UK), which was used for a later measurement on the Gastrolyzer device. Measurements were performed according to the manufacturer's instructions. Participants, who exhaled more than 5 ppm CH₄, were considered as high CH₄ emitters based on (21) and were asked to provide a stool sample and personal data including their health status. For anaerobic cultivation the stool samples were collected with eSwabsTM (Copan, USA) and from the same source for metagenomics with a sterile stool sample container (Sarstedt, AUT). The stool sample container was pre-filled with 5 ml DNA/RNA free ethanol to stabilize the samples, as described earlier (26).

The participants were asked to return the samples within 24 hours after collection and store them at 4 °C in the meantime. After delivery, the samples for anaerobic cultivation were immediately transferred into sterile anoxic (N₂) serum bottles (Glasgerätebau Ochs Laborfachhandel e.K, GER) with sterile syringes (Injekt-F Solo, B.Braun SE, GER) and the same volume of glycerol containing ascorbic acid (50 % glycerol (v/v), 50 % 1x PBS (v/v), and 1 g/l ascorbic acid) was added. Afterwards,

the samples were mixed by inverting, incubated for one hour at 4 °C and then stored at -80 °C until cultivation. Samples for DNA extraction were transferred in DNA-free 1.5 ml sterile reaction tubes (Eppendorf, GER) and frozen at -80°C until further processing.

Microbiome profiling of the original samples

The DNA of the original stool samples was isolated using the PureLink™ Microbiome DNA Purification Kit according to manufacturer's instructions (Invitrogen, Thermo-Fisher, USA).

Shotgun sequencing was conducted by the company Macrogen using the Illumina HiSeq device. Raw sequencing reads were quality filtered with ATLAS (version 2.16.2) which also included the removal of human reads (27). For taxonomic annotation the following tools were used: Kraken2 (version 2.1.2; with a conf. 0.1) and Bracken (version 2.7; read length 100) (28,29). To complete the hierarchical lineage information the script “kreport2mpa.py” was used that is publicly available at github (<https://github.com/jenniferlu717/KrakenTools/blob/master/kreport2mpa.py>) before merging the feature tables of all samples.

General workflow of enrichment and cultivation

Selection of bacterial syntrophy partners and metabolic modelling

Metabolic modeling was used to test the suitability of bacterial syntropy partners on MS (30) and MpT1 (31,32) media for enrichment of *Methanobrevibacter smithii* (full recipes are available in (33)).

Draft metabolic models were generated using gapseq (v1.2) (34) on the genomes of the *B. thetaiotamicron*, *C. minuta* and *M. smithii* (GenBank IDs NC_004663.1, GCF_001652705.1 and ABYW00000000.1, respectively). The recipes for MS and MpT1 media were used to build a representation of media constituents in the ModelSEED (35) namespace. The compositions of the undefined media ingredients yeast extract and casein hydrolysate were approximated using the definitions of yeast extract and tryptone by Marinos et al. (36). The initial models were gap-filled with gapseq on each of the media separately, including the respective nutrient additives for *C. minuta* and *B. thetaiotamicron*.

For the simulations of the co-cultures, PyCoMo (37) was used to build community metabolic models for each pair of organisms in each medium. The respective medium with bacterial additives were applied to the models. Growth of the communities was calculated at equal abundance of bacteria and *M. smithii*. Exchange metabolites and cross-feeding interactions were calculated from solutions of flux balance analysis with the same parameters.

Cross-feeding interactions profiles (metabolites produced by organism A and consumed by organism B in a given co-culture) were compared by calculating the fraction of the intersection of cross-fed metabolites divided by the union of cross-fed metabolites in two given profiles.

Cultivation

A general workflow of the enrichment process is shown in [Fig. 1](#) and detailed flowcharts for each sample can be found on our github repository (https://github.com/SDMUG/Methanobrevibacter_Enrichment). For the enrichment of methanogenic archaea, stool samples were gently thawed on ice and cultivated using following two approaches: i) First, the samples were inoculated in MS and MpT1 media supplemented with antibiotics (0.1 mg/ml penicillin G potassium salt (Carl Roth GmbH + Co. KG, GER) and 0.1 mg/ml streptomycin sulfate (Carl Roth GmbH + Co. KG, GER) to reduce bacterial growth. ii) For the second approach the samples were additionally inoculated in MS and MpT1 media with already growing bacterial cultures (purchased from Leibniz Institute DSMZ - German Collection of Microorganisms and Cell Cultures GmbH, GER) either *Bacteroides thetaiotaomicron* (DSM 2079) or *Christensenella minuta* (DSM 22607); which were described to support the growth of the methanogenic archaea (22,23).

Inoculation for this approach was performed as described in (23). For the cultivation, both media were prepared under anaerobic conditions. In case of cultures with *B. thetaiotaomicron*, the following supplements were additionally added before inoculation to MS and MpT1 media, following the instructions of the DSMZ for the growth of *B. thetaiotaomicron* (medium 78 + haeme + Vit K1, <https://www.dsmz.de/collection/catalogue/details/culture/DSM-2079>): 0.2 ml hemin solution (50 mg hemin; Sigma-Aldrich, USA) in 1 ml 1 M NaOH (Carl Roth GmbH + Co. KG, GER), diluted to 100 ml with ddH₂O; 0.2 ml vitamin K1 solution (0.1 ml vitamin

K1 (Alfa Aesar GmbH & Co KG, GER) in 19 ml 95% (v/v) ethanol (Avantor Performance Material Deventer, NLD)) and 1 ml beef extract solution [100 µg/ml] (MP Biomedicals, USA). In case of *C. minuta*, the media were supplemented with 0.4 ml D-glucose solution [500 µg/ml] (Amresco Inc., USA). All supplements were also prepared under anaerobic conditions and pressurized with 1.0 bar N₂.

The cultures were subjected to incubation at a temperature of 37°C using an incubation shaker set at a shaking speed of 80 rpm. The growth of archaea was influenced by the medium and the presence of supporting bacteria. The incubation period ranged from 7 to 14 days.

The cultures from both approaches were screened for methane and F₄₂₀-positive cells. In the case of approach two, screening occurred prior to FACS sorting, as the sorting process was based on F420 autofluorescence of the methanogens.

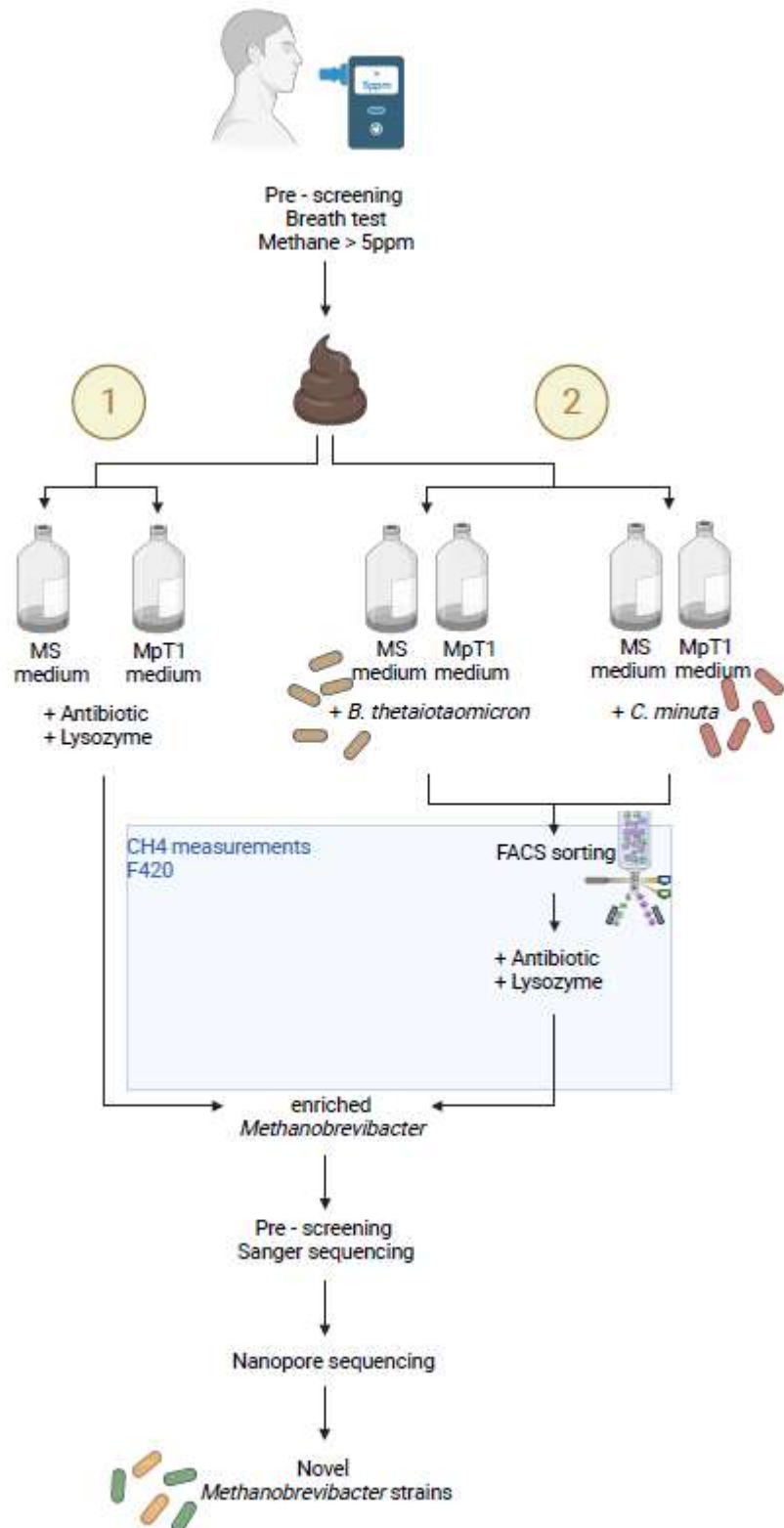


Figure 1: General workflow of the enrichment process.

CH₄ measurement and fluorescence microscopy

To detect the presence of methanogens, the CH₄ sensor BCP-CH₄ (BlueSens gas sensor GmbH, GER) was used to measure CH₄ in the gas phase of the culture bottle according to the manufacturer's manual. Any cultures with CH₄ levels above 2 % were classified as CH₄ positive.

The presence of methanogens was further checked via the typical fluorescence of coenzyme F₄₂₀. For this purpose, fluorescence microscopy (Zeiss microscope Axio Imager A1, Carl Zeiss AG, GER) with fluorescence upgrade was used with Zeiss filter set 05: BP 395-440 (excitation), FT 460 (beam splitter), LP 470 (emission) and 100x magnification (objective Plan-NEOFLUAR).

Fluorescence activated cell sorting (FACS)

To physically enrich the methanogens within the samples, the fluorescence activated cell sorting (FACS) was used on CH₄-positive cultures grown with *B. thetaiotaomicron* or *C. minuta*. Sorting was conducted via the Core Facility Flow Cytometry at the Center of Medical Research in Graz, Austria with FACSariaTM IIu system (BD Biosciences, USA) as described before (38). Prior to sorting, samples were prepared in an anaerobic chamber (Whitley A95 Anaerobic Workstation, Don Whitley Scientific Limited, UK) as follows: 1 ml of culture was centrifuged at 4000 x g for 5 min in a 1.5 ml reaction tube (Eppendorf AG, Hamburg, GER), and the resulting cell pellet was washed twice with 500 µl 1x PBS containing 1 g/L L(+) -ascorbic acid (AppliChem GmbH, GER). The cell pellet was then resuspended in 1 ml of 1x PBS + ascorbic acid and further diluted with an additional 1 ml of 1x PBS + ascorbic acid and transferred to a Falcon® 5 ml Polystyrene Round-Bottom Tube with 35 µm Cell-Strainer Cap (Corning Science Mexico S.A. de C.V., MEX) before sorting to ensure a single cell suspension.

Cells were sorted based on the autofluorescence of coenzyme F₄₂₀ (excitation wavelength at 420 nm) based on (39). F₄₂₀-negative and F₄₂₀-positive cells were distinguished using a 405 nm laser for excitation and a 450/50 band pass filter for detecting fluorescence emission. The presence of autofluorescent cells was observed in CH₄-positive cultures in contrast to its absence in CH₄-negative cultures. In addition, original stool samples, enrichment cultures, and pure cultures of various

methanogenic archaea (*Methanobrevibacter smithii* (DSM 2375), *Methanospaera stadtmanae* (DSM 3091), and *Methanomassiliicoccus luminyensis* (DSM 25720)) were employed for identifying the sorting gate (Supplementary Figures S1- S4). The sort time was chosen for each culture individually and ranged between 3 and 7 minutes, depending on the archaeal cell count.

Sorted cells (min. 800 events, details for each sample can be found in the flowcharts on our github repository) were transferred into a 1.5 ml microcentrifuge tube containing 250 μ l of 1x PBS + ascorbic acid and inoculated into fresh medium. Afterwards the cultures were incubated at 37°C with 80 rpm shaking speed.

Antibiotics, Lysozyme, Dilution series

To reduce bacterial growth and enrich methanogens within the cultures without the addition of *B. thetaiotaomicron* or *C. minuta* and cultures after FACS, antibiotics (penicillin G potassium salt (0.1 mg/ml) and streptomycin sulphate (0.1 mg/ml) were added to the media directly before sample inoculation. For further reduction of antibiotic resistant bacteria, lysozyme (0.5 mg/ml; all substances: Carl Roth GmbH + Co. KG, GER) was added after each culture transfer.

For further purification of the methanogens, dilution series from 10^{-1} - 10^{-13} were performed under anaerobic conditions. Growth was usually observed up to a dilution of 10^{-7} and 10^{-8} . After one week of incubation (37 °C, 80 rpm shaking speed) the CH₄ levels of positive growth cultures were measured and cultures were evaluated further via fluorescence microscopy.

Sequencing and sequence data analysis

Two sequencing approaches were followed to assess the composition of the cultures. Sanger sequencing was used to identify the (almost) pure archaeal and bacterial components of enrichment cultures, whereas Nanopore whole genome sequencing was used for a detailed assessment of metagenomic composition and genome reconstructions. Details are given in the Supplementary Information file.

Scanning electron microscopy (SEM)

The cell morphology of the enriched archaea and their remaining co-existing bacteria was visualized using the Zeiss Sigma 500 VP scanning electron microscope (Carl Zeiss AG, GER). Culture samples of 2 ml (with the supernatant not removed) were centrifuged at 4000 x g for 10 minutes, and the resulting pellets were handed over to the Core Facility Ultrastructure Analysis from Medical University of Graz (Austria) for SEM preparation. Briefly, the cells were mounted on coverslips, fixed with 2 % (wt/vol) paraformaldehyde in 0.1 M phosphate buffered saline, pH 7.4 and 2.5% glutaraldehyde in 0.1 M phosphate buffered saline, pH 7.4, and dehydrated stepwise in a graded ethanol series. Samples were post fixed with 1 % osmium tetroxide (Electron microscopy Sciences) for 1 h at room temperature and subsequently dehydrated in graded ethanol series (30-96 % and 100 % (vol/vol) EtOH). Further, HMDS (Merck | Sigma - Aldrich) was applied. Coverslips were placed on stubs covered with a conductive double coated carbon tape (40). SEM micrographs were taken with an electron voltage of 5 keV and a magnification of 3-21 kX, using the secondary electron detector (Zeiss Oberkochen).

Tree calculation, correlations and pangenome analysis

The ANI (average nucleotide identity) matrix of the genomes (all-vs-all) were calculated using the ANI Matrix calculator provided through (<http://envomics.ce.gatech.edu/g-matrix/>); the resulting phylogenetic tree was annotated using itol (41).

Correlation heatmaps were generated in R. All scripts are provided in our github repository (https://github.com/SDMUG/Methanobrevibacter_Enrichment). Statistical associations were based on spearman correlations, which are also included in the provided script.

Pangenome analyses was performed using kbase (42) based on RastK annotation, the Compute Pangenome and Pangenome Circle Plot (v1.2.0) function, including all available high-quality (> 90% completeness and < 10% contamination) *M. smithii* and *Cand. M. intestini* genomes (this study and (2)), with genomes of Gut_genome132205 and Gut_genome143185 serving as reference genomes.

Genomic, functional annotation and prediction using DeepFRI

Genome comparison was performed using drep v3.4.2 (43), and genome annotation was carried out using eggNOG-mapper v2.1.10 (default settings (e-value cut-off 0.001) (44–49). Prodigal was used for gene identification.

To examine the functional differences between *M. smithii* and *Cand. M. intestini* as well as to explore the differences between functions related to a specific health condition, PCoA were performed using a Bray-Curtis distance matrix. The visualization was done using the R package ggplot2 (50). PERMANOVA was performed with n=999 permutations to identify statistical significance in the functional profiles.

For identifying the functions of protein-coding genes in archaeal genomes, protein-coding genes were first predicted using Prodigal (<https://github.com/hyattpd/Prodigal>). Then, gene sequences translated to amino acids were annotated using a metagenomic pipeline (<https://github.com/bioinf-mcb/Metagenomic-DeepFRI/>) with embedded DeepFRI tool (51). The pipeline generated a query contact map using results from mmseqs2 target database (<https://github.com/soedinglab/MMseqs2>) searching for similar protein sequences with known structures. Next, the contact map alignment was performed to use it as input to DeepFRI Graph Convolutional Network (GCN) and annotations without matches to known structures were processed with Convolutional Neural Network (CNN). DeepFRI version 1.1 was used in this study; in version 1.1 we retrained the original DeepFRI architecture using high-quality models from the AlphaFold Database, thus increasing the number of functions the method can predict by up to 4x (52). For medium quality (MQ) and high quality (HQ) annotation, scores higher than or equal to 0.3 and 0.5 were used, respectively. For selected genes, a structure prediction was performed using AlphaFold database (52,53), followed by DeepFRI annotation (https://github.com/SDMUG/Methanobrevibacter_Enrichment). Wordclouds were generated using the pip package (<https://pypi.org/project/wordcloud/>).

Results

Set-up of a cultivation workflow and selection of bacterial syntrophic partners based on *in silico* predictions

For the cultivation of archaea from human fecal samples, we followed a combined strategy of: i) Providing *in silico*-customized media, partially including selected bacterial syntrophic partners to facilitate *Methanobrevibacter* growth, ii) pre-selection of sample donors for CH₄ exhalation and such a higher methanogen load, iii) rigorous and standardized screening of enrichments for CH₄ production and presence of (unique) methanarchaeal key genes, and iv) FACS and antibiotic treatment for the mechanical and chemical enrichment of methanogens from the bacterial background of syntrophic partners or fecal samples. An overview of this strategy is provided in Fig. 1.

C. minuta and *B. thetaiotaomicron* were selected as potential bacterial syntrophic partners, based on previous reports of successfully established co-cultures with *Methanobrevibacter* species (22,23), and the observed co-occurrence in metagenomic datasets (21). Both species, *C. minuta* and *B. thetaiotaomicron*, were reported to provide hydrogen, acetate and possibly other metabolites to the archaeal partners, with *C. minuta* reported to be more efficient than *B. thetaiotaomicron* (23). Nevertheless, we performed a more detailed prediction of the metabolic capacities of both bacteria to serve as a potential syntrophic partner for *Methanobrevibacter* species.

Metabolic models were generated for *M. smithii*, *C. minuta* and *B. thetaiotamicron*, based on their genomes. At this early stage, *Cand. M. intestini* was not included in the simulations. Single and co-cultures with MS and Mpt1 media were simulated using flux balance analysis (FBA). Across all simulated co-cultures, the growth rate of *M. smithii* was increased compared to the single cultures on the same medium.

This growth boost is enabled by cross-feeding (Supplementary Fig. S5). Multiple metabolites could be identified as mediators of these interactions: The bacteria commonly provided H₂, amino acids (alanine, lysine, glutamine, cysteine), nucleobases and nucleosides (uracil, inosine, adenosine, deoxyguanosine, xanthosine), vitamins and coenzymes (menaquinone 7, coenzyme A, NAD), as well

as fructose, glycerol, formate, putrescine and ethanol (all output files are provided in our github repository). Based on the simulations, both *B. thetaiotamicron* and *C. minuta* were predicted to be fitting partners for *M. smithii*, without clear preference for either. As such, both bacteria and both media were selected for the enrichment cultures.

FACS was established based on the autofluorescence of coenzyme F₄₂₀ (39). Stool samples, and also methanogenic reference strains (see Materials and Methods) were used to identify the optimal sorting conditions, which were then applied to enrichment cultures.

Efficient enrichment of novel *Methanobrevibacter* from donors with detectable archaeal microbiome signatures

Fecal samples from all 16 study participants ([Supplementary Table S1](#)) were processed for enrichment of methanogenic archaea using suitable media with and without additionally added bacteria (see workflow overview [Fig. 1](#)). Overall, 8/8 samples of the healthy cohort and 6/8 of the diseased cohort yielded CH₄-positive cultures (88% of all samples). Some samples yielded several enrichment cultures by different approaches (e.g. P15 and P86).

After initial pre-selection for unique methanarchaea (according to their *mcrA* gene sequence) of all CH₄-positive cultures, enrichment cultures of 14 participant samples were processed further ([Table 1](#)). FACS and visual monitoring for potential purity was performed, and after a minimum of 20 transfers they underwent Nanopore-based whole genome sequencing. An overview of the cultivation workflow and sequencing results (including taxonomic classification through kraken2/bracken) for each individual sample is provided on our github repository.

At this stage, 12 of 16 enrichment cultures were dominated by *Methanobrevibacter* representatives. In more detail, eight were predominated by *M. smithii*, and three by *Cand. M. intestini*. Further, two bacteria-dominated enrichment cultures (P51 and P46) contained a substantial amount of *Cand. M. intestini* ([Fig. 2](#)).

Notably, the dominance of either methanarchaeon was evident in the original microbiome profiling. Samples where *Cand. M. intestini* was predominant in the profiling, exhibited similar dominance of this microbe in subsequent cultivation

attempts. Remarkably, both *Methanobrevibacter* species were present in all samples initially. Yet during the enrichment process, one of these archaea emerged as the predominant species, consistent with their original relative abundance (Table 1). However, in the case of sample P86, we achieved successful enrichment of both *Methanobrevibacter* species separately (Fig. 2).

Table 1: Overview of participants, their health status, the derived cultures and the outcome of the metagenomic profiling of the original fecal sample. CD: Crohn's Disease, IBS: Inflammatory Bowel Syndrome, Lactose I: Lactose intolerance, Fructose I: Fructose intolerance, SIBO: Small Intestinal Bacterial Overgrowth. CH₄ analysis indicated the presence of methanogenic archaea in the participant's microbiome. Derived cultures are labeled according to the participant number, the culture medium (MS: MS medium, MpT1: MpT1 medium), and the supplementation with *B. thetaiotaomicron* (B.t.). Additional genomes acquired through dilution series are annotated with +DS. The predominant archaeon as detected through Nanopore sequencing is given, and the outcome of the CH₄ measurement of the cultures 10 days of incubation at 37°C. The metagenomic information of the original fecal sample was analyzed with respect to the relative abundance of Bacteria, Archaea, *M. smithii* and *Cand. M. intestini*.

PARTICIPANTS			CULTIVATION			METAGENOMIC PROFILING				
#	Disorder	breath CH4 [ppm]	Cultures	Predominant archaeon	CH4 [%]	Bacteria [%]	Archaea [%]	<i>M. smithii</i> [% of archaea]	<i>Cand. M. intestini</i> [% of archaea]	
P15	None	30	P15 (MpT1 / B. t.)	<i>M. smithii</i>	16.5	99.76	0.24	88.8	5.1	
			P15 (MS / B. t.)	<i>M. smithii</i>	20.7					
P20	None	17	P20 (MS / B. t.)	<i>M. smithii</i>	22.2	99.82	0.18	76.5	3.5	
P31	None	70	P31 (MS / B. t.)	<i>M. smithii</i>	23.6	n.a.				
P32	None	44	P32 (MS / B. t.)	<i>M. smithii</i> + DS	23.4	99.87	0.13	90.8	6.3	
P45	None	16	P45 (MS / B. t.)	<i>Cand. M. intestini</i>	23.8	99.84	0.16	7.9	79.5	
P46	None	21	P46 (MpT1 / B. t.)	<i>Cand. M. intestini</i>	24.2	99.49	0.51	8.6	89.9	
P51	None	28	P51 (MS / B. t.)	<i>Cand. M. intestini</i>	5.5	99.96	0.04	6.5	83.1	
P82	None	22	P82 (MpT1)	<i>Cand. M. intestini</i>	25.2	n.a.				
P34	CD, flatulence, abdominal pain	22	n.a.	n.a.	n.a.	n.a.				
P48	IBS	26	P48 (MpT1 / B. t.)	<i>M. smithii</i>	22.2	99.66	0.34	94.0	5.3	
P61	IBS, Lactose I, SIBO	21	P61 (MpT1)	<i>M. smithii</i>	23	n.a.				
P66	Lactose I	55	P66 (MS / B. t.)	<i>M. smithii</i> <i>Cand. M. intestini</i>	21.8	99.16	0.84	94.6	4.8	
P85	CD	6	n.a.	n.a.	n.a.	99.99	0.01	0	0	
P86	Lactose intolerance	13	P86 (MS / B. t.)	<i>Cand. M. intestini</i> + DS	22.4	99.99	0.01	63.9	3.8	
			P86 (MS)	<i>M. smithii</i> + DS	21.1					
P88	IBS, lactose I, fructose I	8	P88 (MS)	<i>M. smithii</i>	22.3	99.87	0.13	72.4	3.8	
P89	IBS, lactose I, pancreatic inflam.	10	P89 (MS / B. t.)	<i>Cand. M. intestini</i>	21.2	99.78	0.22	5.6	88.6	

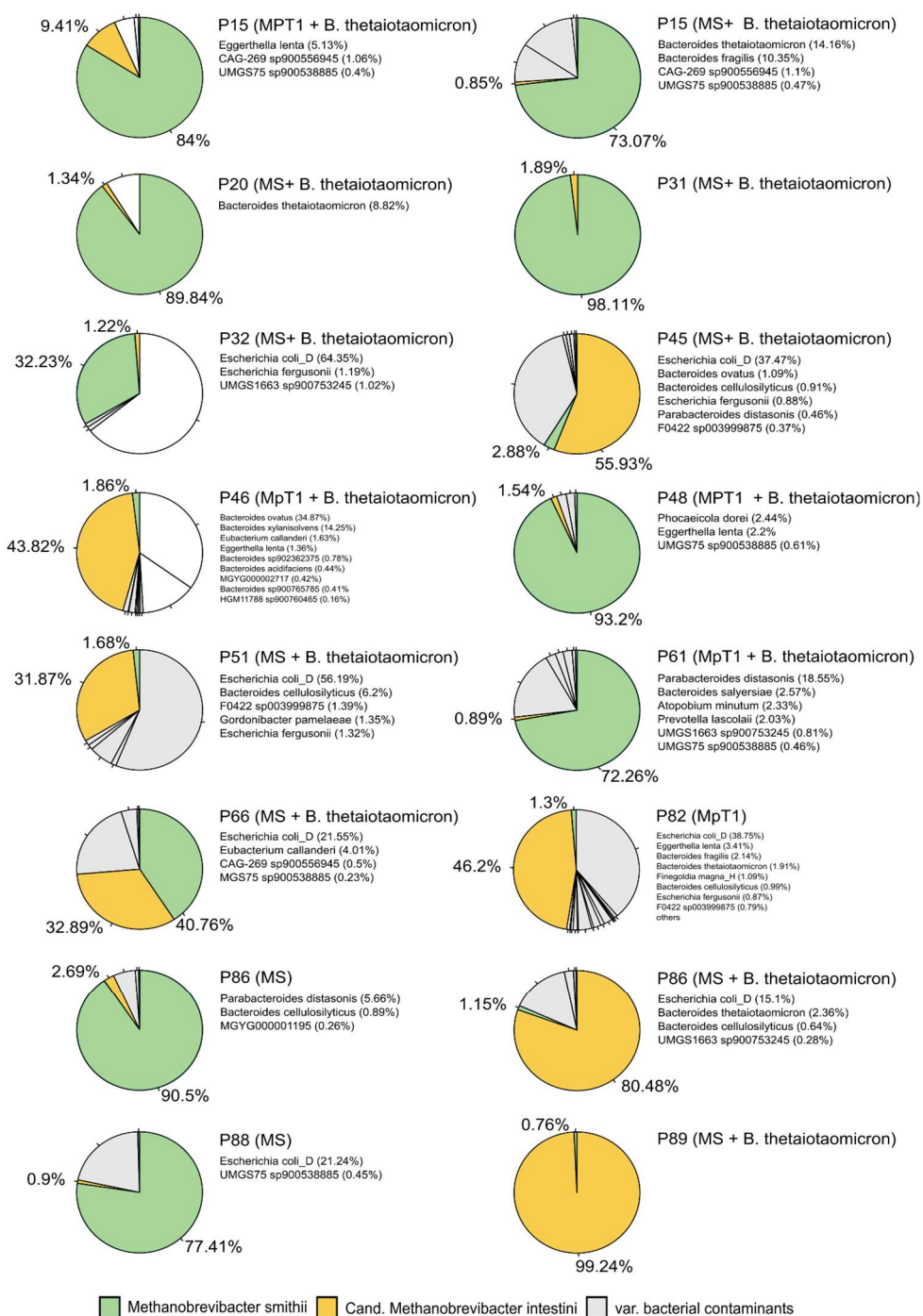


Figure 2: Classified taxa and their relative abundance by Kraken2/bracken output with confidence score of 0.3, before dilution series. *M. smithii* is shown in green and *Cand. M. intestini* in yellow. All original bracken reports are provided in our github repository.

Noteworthy is the observation that samples P34 and P85 failed to yield archaeal cultures, despite positive methane breath test results of the donors (Table 1). While microbiome profiles were accessible for P85 (P34 had to be excluded due to technical reasons), it was evident that this individual lacked archaeal signatures, suggesting an alternative source of methane production, such as undetected methanogens in the oral cavity or small intestine. It shall be noted that these two individuals were the only ones with Crohn's disease included in this study. It is indeed known that Crohn's disease patients have a reduced amount of archaea in their GIT (54).

To further purify the obtained enrichments and obtain monocultures of the methanogens, subsequent dilution series were and are being performed in combination with consequent antibiotics and lysozyme treatment (see Materials and Methods), leading to a substantial improvement of culture purity later on (e.g. P32: from 32.23 % *M. smithii* to 95.05 %; P 86 (MS + B.t.): from 80.48 % *Cand. M. intestini* to 98.4 %; Supplementary Table S3). Enrichment culture P45 (*Cand. M. intestini*) has meanwhile been obtained as a pure culture.

We further visually examined the enrichments with Scanning Electron (SEM) and fluorescence microscopy. The SEM micrographs revealed the presence of mainly short rods (single or in chains) in each of the enrichment cultures, representing the known morphology of *Methanobrevibacter* species. Some rods appeared very bloated, as shown in Fig. 3 (arrows). All cultures were dense and revealed the presence of numerous, actively dividing cells. In agreement with the SEM examinations, we observed cells with *Methanobrevibacter*-typical morphology displaying the F₄₂₀ autofluorescence in all cultures (Supplementary Figure S6).

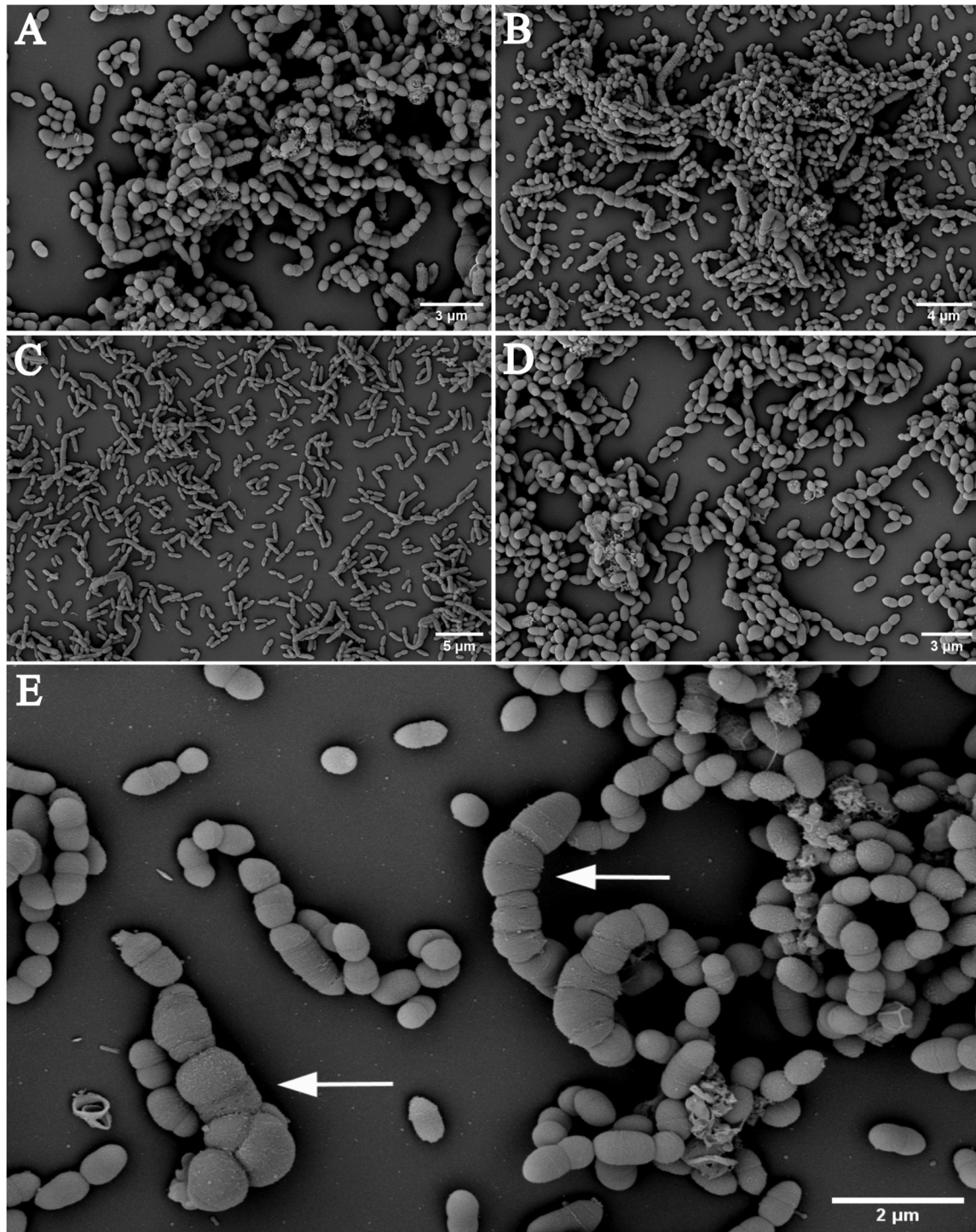


Figure 3: SEM micrographs visualizing the cell morphology of enriched archaeal cultures (*M. smithii*, *Cand. M. intestini*) with co-enriched background bacteria. A: enrichment culture P86, predominated by *M. smithii*. B: enrichment culture P89, predominated by *Cand. M. intestini*. C: enrichment culture P31, predominated by *M. smithii*. D: enrichment culture P51, presence of *Cand. M. intestini*. E: enrichment culture P86 (MS + B.t.), predominated by *Cand. M. intestini*, enlarged for better visibility of different cell phenotypes. Some rods appear bloated (arrows).

Bacteroides thetaiotaomicron, but not *Christensenella minuta*, is a potent syntrophic partner for selective archaeal enrichment

Methane, being uniquely produced by methanogens, serves as an indicator for their presence in cultures. We noted the presence of CH₄ in cultures grown in MS medium with and without supplementation with *B. thetaiotaomicron* after four days of incubation. Similarly, CH₄ was detected in cultures grown in MpT1 medium, with or without supplemental *B. thetaiotaomicron* albeit only after 10 days of incubation.

The addition of *B. thetaiotaomicron* demonstrated a beneficial impact on the efficiency of our enrichment approach. Its presence either had no discernible effect on methanogen enrichment (as evidenced by 12 out of 16 positive enrichment experiments with or without *B. thetaiotaomicron* concurrently) or resulted in an additional strain (P66) not obtained in the abiotic medium (Fig. 2).

However, cultures with additionally added *C. minuta* always remained CH₄ negative (up to 8 weeks of incubation). Also, no autofluorescence of coenzyme F₄₂₀ could be detected for these cultivation attempts. This finding was unexpected, as *C. minuta* had been described as an efficient syntrophic partner of *M. smithii* (23) and we had originally expected positive effects in supporting the growth of these methanogens by providing *C. minuta* in the medium.

Co-enriched bacteria give indications on bacterial partners within the gastrointestinal microbiome

Methanobrevibacter species were enriched with background bacteria from the fecal samples. Interestingly, enrichment cultures with a predominance of *M. smithii* (Supplementary Figure S7) showed only a few significant, weakly positive correlations with specific background bacteria, such as *Phocaeicola dorei* ($q=0.022052$; $r_s=0.3641$) and UMGS75 sp900538885, a so-far uncultivated Bacilli ($q=1.389*10^{-9}$; $r_s= 0.4242$; Spearman correlation and Benjamini Hochberg correction).

A number of negative associations of *M. smithii* were observed, including all *Bacteroides* (e.g. *B. cellulosilyticus*, $q=3.2267*10^{-6}$; $r_s=-0.4112$) and *E. coli* species (e.g. *E. coli_D*, $q=7.8638*10^{-8}$; $r_s= -0.4926$). These were, however, significantly

positive with *Cand. M. intestini* (*B. cellulosilyticus*, $q=0.002058$; $rs= 0.4828$; *E. coli_D*, $q=0.002042$; $rs= 0.2172$; [Supplementary Table S4](#); [Supplementary Fig. S7A](#))

Actually, in all found significant associations ([Supplementary Fig. S7B](#)), the *Methanobrevibacter* species showed opposed preference for bacterial partners, indicating a somewhat different niche preference in the gastrointestinal setting. Also, *M. smithii* showed numerous negative correlations, whereas *Cand. M. intestini*, showed mostly positive correlations to co-cultivated bacteria ([Supplementary Fig. S7B](#)).

Notably, *B. thetaiotaomicron*, although provided in the culture flasks to allow enrichment, was no longer predominant at later stages of the cultivation, indicating that the beneficial effect was rather on pre-priming the medium for methanogenic growth, which was also visible via the faster growth of *Methanobrevibacter* (increased CH₄ content after four days of incubation).

Although both methanarchaeal species (*M. smithii* and *Cand. M. intestini*) co-exist in original gastrointestinal samples (3), their growth in the enrichment cultures was significantly negatively correlated (Spearman correlation, $rs= -0.6559$, $q=1.967059*10^{-7}$), indicating a competitive behavior, at least under the cultivation conditions applied.

Cultured archaea represent nine novel, thus far uncultivated *Methanobrevibacter* strains

From all enrichment cultures, the respective archaeal genomes could be recovered by Nanopore sequencing and genome assembly (see Material and Methods). A summary of the genome classification according to the GTDB database, as well as the checkM2 output representing genome completeness and contamination can be found in [Supplementary Table S5](#). The obtained genomes were placed in the context of available genomes from human-associated *Methanobrevibacter* strains for further analysis (2) (list of genomes provided in [Supplementary Table S6](#); all genome sequences are available through our github repository).

In general, we preserved genomes from nine *M. smithii* and eight *Cand. M. intestini* strains. From the *Cand. M. intestini* clade, we obtained overall four different strain-clusters (cutoff: 99% similarity; Figure 4; MIC-1 to MIC-4), while five clusters were obtained from the *M. smithii* clade (MS-1 to MS-5). All of these clades, except one (MIC-1) represent so far unknown genomes (below 99% identity compared to 1,167

genomes available; ANI values and matrix are given in Supplementary Table S7-S8; (2)). All strains had no cultivated representative thus far, indicating that our enrichment strategy is well suited to expand the cultivable *Methanobrevibacter* diversity.

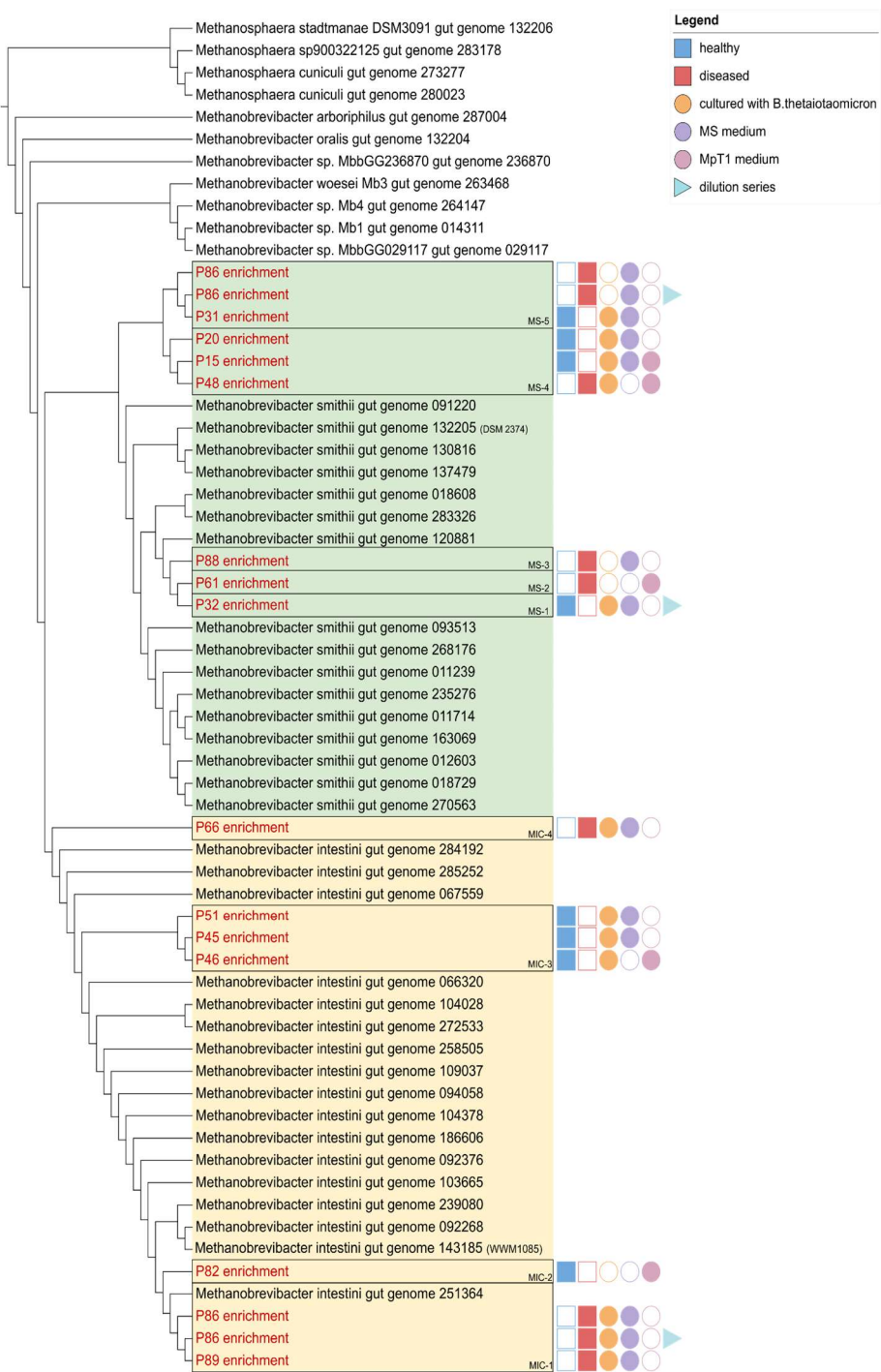


Figure 4: Maximum Likelihood phylogenetic tree calculated based on ANI, retrieved by the comparison of all cultured *Methanobrevibacter* (red letters) and already available genomes from isolates and MAGs (Supplementary Table S6). The *M. smithii* clade is indicated with a green background color; the *Cand. M. intestini* is shown with yellow background color. Cultures are accompanied by additional information on their source (healthy/ diseased donor, and culture conditions). Clusters representing one strain are indicated by black boxes (Supplementary Table S8).

Differences of *Methanobrevibacter smithii* and *Candidatus Methanobrevibacter intestini* isolates revealed through sequence- and structure-based annotation

M. smithii and *Cand. M. intestini* show various differences in their genomic inventory (2). Based on the sequence-based annotation obtained through eggNOG profiling, our findings here corroborate this observation. Including only high-quality genomes (> 90% completeness and < 10% contamination), we identified a significantly different functional profile (PERMANOVA, $F_t = 2.2927$, $R^2 = 0.12533$, $Pr(>F) = 0.002$) among our enriched *Methanobrevibacter* representatives, clearly separating the two species (Supplementary Fig.S8). The analysis included reference genomes of *M. smithii* (Gut_genome132205; DSM2374) and *Cand. M. intestini* (Gut_genome143185; WWM1085; Supplementary Table S6-7).

The most discriminative genes of all obtained genomes (present in $\geq 90\%$ or $\leq 10\%$ of the genomes) are shown in Table 2.

Table 2: Summary of the most discriminative genes found in genomes of *M. smithii* and *Cand. M. intestini*. Table shows counts and percentages of genomes in which the respective function is present. Distinguishing characteristics derived from high-quality genomes are emphasized in bold. P: Inorganic ion transport and metabolism, I: Lipid metabolism, S: Function unknown, K: Transcription, F: Nucleotide transport and metabolism, G: Carbohydrate transport and metabolism, C: Energy production and conversion, H: Coenzyme transport and metabolism, Q: Secondary metabolites biosynthesis, transport and catabolism. N.d.: not done. **: High quality annotation (annotations with score ≥ 0.5); *: medium quality annotation (annotations with score ≥ 0.25)

eggNOG orthologous groups	Prevalence in <i>M. smithii</i> genomes		Prevalence in <i>Cand. M. intestini</i> genomes		COG category	Genomic annotation (EggNOG)	Functional annotation (DeepFri)
	count (total/present)	present in % of genomes	count (total/present)	present in % of genomes			
COG0725	12/12	100	0/10	0	P	ABC-type molybdate transport system, periplasmic component (<i>modA</i>)	ion binding (GO:0043167)**
COG4149	12/12	100	0/10	0	P	ABC-type molybdate transport system, permease component (<i>modB</i>)	regulation of metabolic process (GO:0080090)*/**; catalytic activity (GO:0003824)**; membrane-associated (GO:0016020)**
2EI95	12/12	100	1/10	10	F/G	unknown function	nucleotide-sugar transmembrane transporter activity (GO:0005338) **
COG4925	11/12	91.67	1/10	10	I	sulfurtransferase activity; cyclophilin-like domain-containing protein	transferase activity (GO:0016740)
COG0586	0/12	0	10/10	100	S	Uncharacterized membrane protein DedA, SNARE-associated domain	nd
COG2076	0/12	0	10/10	100	P	Membrane transporters of cations and cationic drugs	nd
arCOG00818	1/12	8.33	10/10	100	S	AbrB family transcriptional regulator	nd
2AVB5	0/12	0	9/10	90	F/G	unknown function	nucleotide-sugar transmembrane transporter activity (GO:0005338)
2C5WB	0/12	0	9/10	90	CHQ	unknown function	oxidoreductase (GO:0016491); oxalyl-CoA decarboxylase activity (GO:0008949)
2DDW5	0/12	0	9/10	90	G	unknown function	glycosyltransferase activity (GO:0016757); oxidoreductase (GO:0016616) involved in the steroid biosynthetic process (GO:0006694)
COG5015	0/12	0	9/10	90	S	Pyridoxamine 5'-phosphate oxidase family	nd
COG1733	0/12	0	9/10	90	K	HxLR-like helix-turn-helix	nd

As typical for archaeal genomes, a high number of proteins cannot be assigned to a function (54% across 1.8 million proteins from 1,167 genomes; (2)), due to missing databases and mechanistic information. For that reason, we performed a structure-based protein function prediction via DeepFRI which is reliant on Alpha-fold (51) for

the most discriminative functions. By doing so, three previously unknown functional genes (2AVB5, 2C5WB and 2DDW5) from *Cand. M. intestini* could be annotated (Table 2). Frequencies of the occurring GO terms in annotations are shown as word clouds in Supplementary Fig. S9.

Most discriminative functions were involved in substrate/ ion transport, such as for molybdate, as all *M. smithii* genomes analyzed in this study carried the *modA* and *modB* subunits for the ABC (molybdate) transporter. *ModA* binds molybdate and tungstate with high affinity, and together with *ModB* transport permease protein is widely distributed across methanogens. Molybdopterin is an important cofactor for the formate dehydrogenase, indicating some difference in the formate metabolism of both species (55). Indeed, differences in the behaviour of formate metabolism in *Cand. M. intestini* was found, as it, in contrast to *M. smithii* strains, accumulated formate in its medium, although the formate dehydrogenase and formate transporters are coded in its genome (33). Further, unique nucleotide-sugar transmembrane transporters for each species were identified through DeepFri annotation.

Another finding was the potential presence of an oxalyl-CoA decarboxylase in the *Cand. M. intestini*; these enzymes are highly important to eliminate oxalates from human diet contained in e.g. coffee, tea and chocolate (56), and would allow for the release of CO₂ and formyl-CoA (<https://www.ebi.ac.uk/QuickGO/>).

Although *Cand. M. intestini* genomes were somewhat larger (1.8 Mbp) compared to *M. smithii* (1.7 Mbp; see also (2)), the overall gene count was similar (~1,900 genes per genome). The percentage of core genes was also very similar (66.39% for *M. smithii*; 66.61% for *Cand. M. intestini*), but variations were observed in the percentage of non-core functions (27.79% and 29.47, respectively) (Supplementary Figure S10). Notably, the representative *Cand. M. intestini* genome (Gut_genome132205) revealed double the amount (n=36) of genes involved in defense mechanisms than the representative genome of *M. smithii* (Gut_genome132205, DSM2374, n=18). The additional genes included mainly CRISPR-associated proteins or genes involved in Type I restriction modification (Supplementary Table S9), indicating a potentially more competitive environment for *Cand. M. intestini* (Supplementary Fig. S11)

Functional annotations indicate potential differences of *Methanobrevibacter* species according donor health status

We explored the functional profiles of the archaeal cultures obtained from both healthy and diseased participants. This analysis excluded all reference genomes due to the unknown health status of the source individuals and thus only initial insights can be retrieved.

Overall, *Methanobrevibacter* genomes of healthy and diseased individuals did not differ significantly (Supplementary Fig. S12, eggNOG annotation), but the *Cand. M. intestini* population revealed variances according to the health status of the respective donor. Some potential unique functions for representatives stemming from the diseased (n=4) and healthy cohort (n=4) could also be identified (Supplementary Table S10). Unique functions found in *Cand. M. intestini* genomes from subjects with gastrointestinal issues were mainly CRISPR-associated proteins (arCOG05124: CRISPR-associated protein TM1802 (cas_TM1802); COG3649: (CRISPR-associated protein Cas7)). Three unresolved annotations (arCOG07602, 2DP7E, 2DQUR) were further tackled through structure-based function prediction and identified functions involved, amongst others, hydrolase activities (Supplementary Fig. S13-14; Supplementary Table S10).

In general, the identified functions (DeepFri) for the unique COGs of *Cand. M. intestini* genomes derived from the diseased participants were mainly related to 5'-3' nuclease activity, RNA polymerase activity and DNA polymerase complex, suggesting the alteration in gene expression, with the metabolic functions being mainly organonitrogen compound biosynthesis and macromolecule metabolism (HQ annotations only; Supplementary Fig. S15).

However, the *Cand. M. intestini* genomes obtained from the healthy cohort revealed a higher number of unique functions, in particular when DeepFRI-based annotation was performed. Annotations exclusive to healthy cohorts included a wider range of functions, e.g. peptidase regulation, lipid metabolism, glycosyltransferase, methyltransferase and nucleotidyltransferase, as well as regulation of signal transduction and cell communication. Other annotations were associated with functions associated with membrane, cytoskeleton and chromatin (Supplementary Fig. S15).

In summary, genes unique to the *Cand. M. intestini* genomes preliminarily identified in the healthy cohort in this study, encode a broad range of functions (cellular processing, metabolism, information storage and processing), whereas genes unique to the diseased cohort were mainly involved in CRISPR activities, DNA and RNA processing (Supplementary Fig. S15), warranting a closer look into this matter with additional cultures and genomes.

Discussion

Despite acknowledging archaea in the human gut microbiome for over 40 years (14), our understanding of their functions and roles are still limited. The major bottleneck is the rare availability of cultivable representatives that would allow for deeper, mechanistic, comprehensive analyses, including multi-omics and interaction studies (57).

Development of an efficient cultivation procedure

In this study, we developed a targeted culturing procedure to efficiently enrich and isolate methanogenic archaea from human fecal samples. This approach enabled the stable cultivation of several *M. smithii* and *Cand. M. intestini* strains from participants with varying health conditions, facilitating genomic and functional comparisons. These cultures include nine previously uncultivated strains, with only one revealing overlap with one of more than 1,000 recently recovered metagenome assembled genomes (2).

From all donors, except Crohn's disease patients, stable methanogen cultures could be recovered, which is a proof of the efficient enrichment pipeline. Such high efficiency could even allow personalized archaeome studies based on individual microbiomes.

Growth inhibition by *C. minuta*

(Human) methanogens often rely on syntropy with bacterial partners that provide small carbon compounds and hydrogen for methanogenesis (58). In particular *Christensenella* and *Bacteroides* species were considered as potent partners, as they generally correlate positively with *Methanobrevibacter* species in natural gut microbiomes, in previous experiments (23) and confirmation through *in silico* modeling (22) (and this study). In our targeted approach, we utilized this positive interaction and added both bacterial species to the culture media in order to induce the low levels of methanogens to grow, as it has been proposed earlier (57). Nevertheless, in contrast to cultures in which *B. thetaiotaomicron* was provided as syntrophic partner, all our enrichment attempts remained methane- and methanogen-negative when *C. minuta* was added, indicating a potential competition under the artificial culture-media conditions, despite their re-current co-existence in natural gastrointestinal microbiomes (3,21). Pre-priming of the media with *B. thetaiotaomicron*, however, was slightly advantageous, as one *Methanobrevibacter* strain could only be cultured with its addition.

Co-enriched bacteria from human GIT microbiome

Besides those known interaction partners, we co-enriched background bacteria from feces, which might give indications on potential, natural bacterial interaction partners

within the GIT microbiome. In contrast to *M. smithii* enrichments, *Cand. M. intestini* was revealing a strong co-occurrence with bacteria, such as *E. coli* and *Bacteroides* species. Both bacterial taxa produce a variety of substances from more or less complex sugar components, such as succinate, formate, acetate, lactate and ethanol (59,60). This indicates a potential dependency of *Cand. M. intestini* on these or other components that are not well provided in the medium, or an inhibition of *M. smithii* by those or other components.

Retrieval of pure cultures

The provision of syntrophic partners, as well as the co-enrichment of bacteria from the original samples results in a minor, but stable background contamination in the enrichment cultures. To obtain final pure cultures, this background contamination has to be removed, by e.g. using optical tweezers, micromanipulators, encapsulation methods or high-throughput single cell isolation (57). In our case, we used a combination of antibiotics/lysozyme treatment and dilution series, which substantially improved the archaeal predominance, and meanwhile led to the first pure isolate of a novel *Cand. M. intestini* strain (P45).

As all enrichment cultures are very stable and maintained for months and >50 transfers in our laboratory now, we also might have to consider that some co-cultures that resist clonal purification, are reliant on the archaeal-bacterial interaction, i.e. by syntropy or any other mechanisms. Co-cultures reflect natural conditions to a greater extent, and creative solutions are needed to still obtain pure cultures (61,62), which are, for example, a prerequisite for the inclusion of these organisms in a culture collection. However, providing these strains to the scientific community is a declared goal, in order to extend the wealth of available *Methanobrevibacter* isolated from the human gut for future mechanistic studies.

Insights into the genomes and advantages of structure-based predictions

M. smithii and *Cand. M. intestini* stand out as distinct species, characterized by unique microbial networks, physiological roles, and genomic potentials (33,63). Like many other archaea, much of their genetic landscape remains unexplored, as a significant portion of their genes lack annotation, and genetic models are yet to be established. To delve deeper into their characteristics, we employed structure-based predictions to complement sequence-based tools for annotation (64). As previously observed (65), also archaeal COG groups when further annotated using DeepFRI (51), exhibit enhanced accuracy and coverage of annotated functions compared to orthodox orthology-based methods. As such, we were able to retrieve a higher resolution in the distinction of *M. smithii* and *Cand. M. intestini* genomes, and identified some novel functions (such as the putative oxalyl-CoA decarboxylase) that could be relevant for the gastrointestinal ecosystem.

The role of methanogenic archaea for health and disease are still a matter of ongoing studies (summarized in (3), and (18)). In particular, the role of *Cand. M. intestini* remains to be explored, as earlier studies could not resolve both species separately, due to the high sequence similarity in the 16S rRNA gene (33). In our study, the number of participants and the subsequent cultures and genomes was quite low, so that a relevance of either species for disease/health cannot be concluded at this stage. Nevertheless, structure-based analyses of the clusters of orthologous groups of the *Cand. M. intestini* genomes revealed some differences based on the health status of the donor, with a broader variety of functions associated with the healthy phenotype, and a number of functions associated with CRISPR, and DNA/RNA processing in the diseased phenotypes, lacking also a clear indication of their subcellular location, which might indicate a potential foreign origin (e.g. phage/virus). These results should be considered as preliminary evidence, showcasing the potential lying in the cultures and genomes, but also emphasizing the need for further investigation.

Conclusion and outlook

In this study, we have successfully extended the cultivable human archaeome through a targeted cultivation approach that relied on a strategic selection of samples and optimized culture conditions including syntrophic bacterial strains. This approach facilitated the growth of *Methanobrevibacter* species, resulting in the stable cultivation of nine novel strains belonging to the two major archaeal species in the human gastrointestinal ecosystem, namely *M. smithii* and *Cand. M. intestini*. The derived genomes can be used to obtain first insights into the physiology and functions that might be relevant for human health or disease.

Furthermore, our method has proven highly efficient, as evidenced by ongoing work in our laboratory, as we were able to enrich methanogens even from individuals with methane content below 5 ppm in their breath. This highlights the robustness of our approach and its potential for widespread application.

Our work opens the way for comprehensive analyses that promise to deepen our understanding of methanogen dynamics within the human gastrointestinal tract. Expanding the public isolate collection is essential for gaining further insights into the roles of methanogens in the human microbiome.

Data availability

All used and created data is made publically available on our github repository:
https://github.com/SDMUG/Methanobrevibacter_Enrichment

Acknowledgments

We want to acknowledge the support of Petra Jurše Kupper and Astrid Koller in the recruitment process, and we thank all donors that have contributed with their samples. This research was funded in whole or in part by the Austrian Science Fund (FWF) [grants P 32697, P 30796, SFB F-83, COE 7, doc.funds project DOC 69]. For open access purposes, the author has applied a CC BY public copyright license to any author-accepted manuscript version arising from this submission. SD and MP were supported by their local doctoral programs MolMed (Medical University of Graz) and the Doctoral School in Microbiology and Environmental Science (University of Vienna).

Conflict of interests

The authors declare no competing interests.

Authors' contributions

The study was designed by SD and CME. Method establishment was done by SD, MB and AE. Recruitment was carried out by SD and supported by LSC, CH and AMM. Sample collection and sample preparation was performed by SD, SV, LSC, and TZ. The samples were cultivated by SD, SV and MD. FACS was done by SD, SV, MD and VZ. AM, CK, SV and MD performed Nanopore sequencing, and SD, AM, LS and CME did data analysis. SD, SV, MD, VW, and CME created the shown figures and micrographs. DK and DP prepared the samples for SEM. MP and TR performed metabolic modeling, LS and TK performed the DeepFRI analyses. SD and CME wrote the manuscript, and SV, TK, RM, RS, MP, and AM contributed to the writing of the manuscript, which was read and approved by all authors.

List of Supplementary Materials

Supplementary Tables (can be found in the github repository)

Supplementary Table S1: Overview of the 16 recruited participants and their metadata

Supplementary Table S2: Overview of inclusion and exclusion criteria for participant recruitment

Supplementary Table S3: Composition of enrichment cultures after antibiotics and lysozyme treatments

Supplementary Table S4: Spearman correlations of co-cultured archaea and bacteria

Supplementary Table S5: Recovered genomes, their classification according to GTDB, completeness and contamination.

Supplementary Table S6: List of *Methanobrevibacter* genomes

Supplementary Table S7: ANI Matrix

Supplementary Table S8: ANI distances from different clusters to themselves and *Candidatus M. intestini* (CMI, WWM1085) and *M. smithii* (MS, DSM2374).

Supplementary Table S9: Kbase annotation output on CRISPR Functions for *M. smithii* (left table) and *Cand. M. intestini* (right table)

Supplementary Table S10: Genomic and functional annotation of genes divergent in *Methanobrevibacter* genomes from diseased and healthy individuals

Supplementary Information and Figures

Supplementary Methods: Sequencing

Supplementary Figure S1: General gating strategy of FACS sorting.

Supplementary Figure S2: FACS sorting: Example of a (A) CH4-negative and (B) CH4-positive culture.

Supplementary Figure S3: FACS Sorting of pure cultures.

Supplementary Figure S4: FACS Sorting of mixed cultures.

Supplementary Figure S5: Comparison of cross-feeding interaction profiles in simulated co-cultures.

Supplementary Figure S6: Light- and corresponding fluorescence micrographs

Supplementary Figure S7A: Clustered heatmap of the relative abundances of archaeal and bacterial taxa in each enrichment culture.

Supplementary Figure S6B: Correlation matrix showing positive (blue dots) and negative correlations with co-enriched bacteria.

Supplementary Figure S7: PCoA, based on the presence/absence matrix obtained through functional annotation

Supplementary Fig. S8. Occurrences of DeepFRI annotations (as Go term annotations) of otherwise unknown functions of *Cand. M. intestini*.

Supplementary Fig. S9: Pangenome circle plot

Supplementary Fig. S10: Inventory of CRISPR-associated genes

Supplementary Fig. S11: Comparison of the genomic inventory (PcoA) of the enriched *Methanobrevibacter* representatives

Supplementary Fig. S12: Occurrences of DeepFRI annotations in diseased cohort

Supplementary Fig. S13: Occurrences of DeepFRI annotations in healthy cohort

Supplementary Fig. S14. Comparison of *Cand. M. intestini* genomes from healthy and diseased cohorts, DeepFRI results.

References

Arkin, A. P., Cottingham, R. W., Henry, C. S., Harris, N. L., Stevens, R. L., Maslov, S., Dehal, P., Ware, D., Perez, F., Canon, S., Sneddon, M. W., Henderson, M. L., Riehl, W. J., Murphy-Olson, D., Chan, S. Y., Kamimura, R. T., Kumari, S., Drake, M. M., Brettin, T. S., ... Yu, D. (2018). KBase: The United States Department of Energy Systems Biology Knowledgebase. *Nature Biotechnology*, 36(7), 566–569. <https://doi.org/10.1038/nbt.4163>

Balch, W. E., Fox, G. E., Magrum, L. J., Woese, C. R., & Wolfe, R. S. (1979). Methanogens: reevaluation of a unique biological group. *Microbiological Reviews*, 43(2), 260.

Bang, C., & Schmitz, R. A. (2015). Archaea associated with human surfaces: not to be underestimated. *FEMS Microbiology Reviews*, 39(5), 631–648. <https://doi.org/10.1093/femsre/fuv010>

Borrel, G., Brugère, J. F., Gribaldo, S., Schmitz, R. A., & Moissl-Eichinger, C. (2020). The host-associated archaeome. In *Nature Reviews Microbiology* (Vol. 18, Issue 11, pp. 622–636). Nature Research. <https://doi.org/10.1038/s41579-020-0407-y>

Buchfink, B., Reuter, K., & Drost, H.-G. (2021). Sensitive protein alignments at tree-of-life scale using DIAMOND. *Nature Methods*, 18(4), 366–368. <https://doi.org/10.1038/s41592-021-01101-x>

Cantalapiedra, C. P., Hernández-Plaza, A., Letunic, I., Bork, P., & Huerta-Cepas, J. (2021). eggNOG-mapper v2: Functional Annotation, Orthology Assignments, and Domain Prediction at the Metagenomic Scale. *Molecular Biology and Evolution*, 38(12), 5825–5829. <https://doi.org/10.1093/molbev/msab293>

Catlett, J. L., Carr, S., Cashman, M., Smith, M. D., Walter, M., Sakkaff, Z., Kelley, C., Pierobon, M., Cohen, M. B., & Buan, N. R. (2022). Metabolic Synergy between Human Symbionts Bacteroides and Methanobrevibacter. *Microbiology Spectrum*, 10(3). https://doi.org/10.1128/SPECTRUM.01067-22/SUPPL_FILE/SPECTRUM.01067-22-S002.XLSX

Chibani, C. M., Mahnert, A., Borrel, G., Almeida, A., Werner, A., Brugère, J.-F., Gribaldo, S., Finn, R. D., Schmitz, R. A., & Moissl-Eichinger, C. (2022). A catalogue of 1,167 genomes from the human gut archaeome. *Nature Microbiology*, 7(1), 48–61. <https://doi.org/10.1038/s41564-021-01020-9>

Dridi, B., Henry, M., El Khechine, A., Raoult, D., & Drancourt, M. (2009). High prevalence of Methanobrevibacter smithii and Methanospaera stadtmanae detected in the human gut using an improved DNA detection protocol. *PLoS One*, 4(9), e7063–e7063.

Eddy, S. R. (2011). Accelerated Profile HMM Searches. *PLoS Computational Biology*, 7(10), e1002195. <https://doi.org/10.1371/journal.pcbi.1002195>

Fricke, W. F., Seedorf, H., Henne, A., Krüer, M., Liesegang, H., Hedderich, R., Gottschalk, G., & Thauer, R. K. (2006). The genome sequence of Methanospaera stadtmanae reveals why this human intestinal archaeon is restricted to methanol and H₂ for methane formation and ATP synthesis. *Journal of Bacteriology*, 188(2), 642–658.

Gaci, N., Borrel, G., Tottey, W., O'Toole, P. W., & Brugère, J.-F. (2014). Archaea and the human gut: New beginning of an old story. *World Journal of Gastroenterology*, 20(43), 16062. <https://doi.org/10.3748/wjg.v20.i43.16062>

Gasińska, A., & Gajewska, D. (2007). Tea and coffee as the main sources of oxalate in diets of patients with kidney oxalate stones. *Roczniki Państwowego Zakładu Higieny*, 58(1), 61–67.

Gligorijević, V., Renfrew, P. D., Kosciolak, T., Leman, J. K., Berenberg, D., Vatanen, T., Chandler, C., Taylor, B. C., Fisk, I. M., Vlamakis, H., Xavier, R. J., Knight, R., Cho, K., &

Bonneau, R. (2021). Structure-based protein function prediction using graph convolutional networks. *Nature Communications*, 12(1), 3168. <https://doi.org/10.1038/s41467-021-23303-9>

Huerta-Cepas, J., Szklarczyk, D., Heller, D., Hernández-Plaza, A., Forslund, S. K., Cook, H., Mende, D. R., Letunic, I., Rattei, T., & Jensen, L. J. (2019). eggNOG 5.0: a hierarchical, functionally and phylogenetically annotated orthology resource based on 5090 organisms and 2502 viruses. *Nucleic Acids Research*, 47(D1), D309–D314.

Hyatt, D., Chen, G.-L., LoCascio, P. F., Land, M. L., Larimer, F. W., & Hauser, L. J. (2010). Prodigal: prokaryotic gene recognition and translation initiation site identification. *BMC Bioinformatics*, 11(1), 119. <https://doi.org/10.1186/1471-2105-11-119>

Jumper, J., Evans, R., Pritzel, A., Green, T., Figurnov, M., Ronneberger, O., Tunyasuvunakool, K., Bates, R., Žídek, A., Potapenko, A., Bridgland, A., Meyer, C., Kohl, S. A. A., Ballard, A. J., Cowie, A., Romera-Paredes, B., Nikolov, S., Jain, R., Adler, J., ... Hassabis, D. (2021). Highly accurate protein structure prediction with AlphaFold. *Nature*, 596(7873), 583–589. <https://doi.org/10.1038/s41586-021-03819-2>

Kaeberlein, T., Lewis, K., & Epstein, S. S. (2002). Isolating “Uncultivable” Microorganisms in Pure Culture in a Simulated Natural Environment. *Science*, 296(5570), 1127–1129. <https://doi.org/10.1126/science.1070633>

Kieser, S., Brown, J., Zdobnov, E. M., Trajkovski, M., & McCue, L. A. (2020). ATLAS: A Snakemake workflow for assembly, annotation, and genomic binning of metagenome sequence data. *BMC Bioinformatics*, 21(1), 1–8. <https://doi.org/10.1186/S12859-020-03585-4/FIGURES/2>

Koehler Leman, J., Szczerbiak, P., Renfrew, P. D., Gligorijevic, V., Berenberg, D., Vatanen, T., Taylor, B. C., Chandler, C., Janssen, S., Pataki, A., Carriero, N., Fisk, I., Xavier, R. J., Knight, R., Bonneau, R., & Koscioletk, T. (2023). Sequence-structure-function relationships in the microbial protein universe. *Nature Communications*, 14(1), 2351. <https://doi.org/10.1038/s41467-023-37896-w>

Kuehnast, T., Kumpitsch, C., Mohammadzadeh, R., Weichhart, T., Moissl-Eichinger, C., & Heine, H. (2024). Exploring the Human Archaeome: Its Relevance for Health, Disease, and its Complex Interplay with the Human Immune System. *The FEBS Journal*, accepted.

Kumpitsch, C., Fischmeister, F. P. S., Mahnert, A., Lackner, S., Wilding, M., Sturm, C., Springer, A., Madl, T., Holasek, S., & Högenauer, C. (2021). Reduced B12 uptake and increased gastrointestinal formate are associated with archaeome-mediated breath methane emission in humans. *Microbiome*, 9(1), 1–18.

Lambrecht, J., Cichocki, N., Hübschmann, T., Koch, C., Harms, H., & Müller, S. (2017). Flow cytometric quantification, sorting and sequencing of methanogenic archaea based on F420 autofluorescence. *Microbial Cell Factories*, 16(1), 180. <https://doi.org/10.1186/s12934-017-0793-7>

Lee, S. J., Lee, D.-Y., Kim, T. Y., Kim, B. H., Lee, J., & Lee, S. Y. (2005). Metabolic Engineering of Escherichia coli for Enhanced Production of Succinic Acid, Based on Genome Comparison and In Silico Gene Knockout Simulation. *Applied and Environmental Microbiology*, 71(12), 7880–7887. <https://doi.org/10.1128/AEM.71.12.7880-7887.2005>

Letunic, I., & Bork, P. (2021). Interactive Tree Of Life (iTOL) v5: an online tool for phylogenetic tree display and annotation. *Nucleic Acids Research*, 49(W1), W293–W296. <https://doi.org/10.1093/nar/gkab301>

Lu, J., Breitwieser, F. P., Thielen, P., & Salzberg, S. L. (2017). Bracken: estimating species abundance in metagenomics data. *PeerJ Computer Science*, 3, e104.

Mahnert, A., Blohs, M., Pausan, M. R., & Moissl-Eichinger, C. (2018). The human archaeome: methodological pitfalls and knowledge gaps. *Emerging Topics in Life Sciences*, 2(4), 469–482.

Maranga, M., Szczerbiak, P., Bezshapkin, V., Gligorijevic, V., Chandler, C., Bonneau, R., Xavier, R. J., Vatanen, T., & Kosciolek, T. (2023). Comprehensive Functional Annotation of Metagenomes and Microbial Genomes Using a Deep Learning-Based Method. *MSystems*, 8(2). <https://doi.org/10.1128/msystems.01178-22>

Marinos, G., Kaleta, C., & Waschyna, S. (2020). Defining the nutritional input for genome-scale metabolic models: A roadmap. *PLOS ONE*, 15(8), e0236890. <https://doi.org/10.1371/journal.pone.0236890>

Mauerhofer, L.-M., Zwirtmayr, S., Pappenreiter, P., Bernacchi, S., Seifert, A. H., Reischl, B., Schmider, T., Taubner, R.-S., Paulik, C., & Simon, K.-M. R. (2021). Hyperthermophilic methanogenic archaea act as high-pressure CH 4 cell factories. *Communications Biology*, 4(1), 1–12.

May, H. D., Patel, P. S., & Ferry, J. G. (1988). Effect of molybdenum and tungsten on synthesis and composition of formate dehydrogenase in *Methanobacterium formicum*. *Journal of Bacteriology*, 170(8), 3384–3389. <https://doi.org/10.1128/jb.170.8.3384-3389.1988>

Miller, T. L., Wolin, M. J., de Macario, E. C., & Macario, A. J. (1982). Isolation of *Methanobrevibacter smithii* from human feces. *Applied and Environmental Microbiology*, 43(1), 227–232.

Mohammadzadeh, R., Mahnert, A., Duller, S., & Moissl-Eichinger, C. (2022). Archaeal key-residents within the human microbiome: characteristics, interactions and involvement in health and disease. *Current Opinion in Microbiology*, 67, 102146. <https://doi.org/10.1016/J.MIB.2022.102146>

Mohammadzadeh, R., Mahnert, A., Shinde, T., Kumpitsch, C., Weinberger, V., Schmidt, H., & Moissl-Eichinger, C. (2024). Age-Related Dynamics of Methanogenic Archaea in the Human Gut Microbiome: Implications for Longevity and Health. *BioRxiv*, 2024.02.09.579604. <https://doi.org/doi: https://doi.org/10.1101/2024.02.09.579604>

Morris, B. E. L., Henneberger, R., Huber, H., & Moissl-Eichinger, C. (2013). Microbial syntrophy: Interaction for the common good. In *FEMS Microbiology Reviews* (Vol. 37, Issue 3, pp. 384–406).

Neal, M., Thiruppathy, D., & Zengler, K. (2023). Genome-scale metabolic modeling of the human gut bacterium *Bacteroides fragilis* strain 638R. *PLOS Computational Biology*, 19(10), e1011594. <https://doi.org/10.1371/journal.pcbi.1011594>

Olm, M. R., Brown, C. T., Brooks, B., & Banfield, J. F. (2017). DRep: A tool for fast and accurate genomic comparisons that enables improved genome recovery from metagenomes through de-replication. *ISME Journal*, 11(12), 2864–2868. <https://doi.org/10.1038/ismej.2017.126>

Paul, K., Nonoh, J. O., Mikulski, L., & Brune, A. (2012). “Methanoplasmatales,” Thermoplasmatales-related archaea in termite guts and other environments, are the seventh order of methanogens. *Applied and Environmental Microbiology*, 78(23), 8245–8253.

Plastira, I., Bernhart, E., Joshi, L., Koyani, C. N., Strohmaier, H., Reicher, H., Malle, E., & Sattler, W. (2020). MAPK signaling determines lysophosphatidic acid (LPA)-induced inflammation in microglia. *Journal of Neuroinflammation*, 17(1), 127. <https://doi.org/10.1186/s12974-020-01809-1>

Polag, D., & Keppler, F. (2019). Global methane emissions from the human body: Past, present and future. *Atmospheric Environment*, 214, 116823.

Predl, M., Mießkes, M., Rattei, T., & Zanghellini, J. (2024). PyCoMo: a python package for community metabolic model creation and analysis. *In Revision*.

Ruaud, A., Esquivel-Elizondo, S., de la Cuesta-Zuluaga, J., Waters, J. L., Angenent, L. T., Youngblut, N. D., & Ley, R. E. (2020). Syntrophy via Interspecies H₂ Transfer between Christensenella and Methanobrevibacter Underlies Their Global Cooccurrence in the Human Gut. *MBio*, 11(1). <https://doi.org/10.1128/mBio.03235-19>

Scanlan, P. D., Shanahan, F., & Marchesi, J. R. (2008). Human methanogen diversity and incidence in healthy and diseased colonic groups using mcrA gene analysis. *BMC Microbiology*, 8(1), 1–8. <https://doi.org/10.1186/1471-2180-8-79>

Seaver, S. M. D., Liu, F., Zhang, Q., Jeffries, J., Faria, J. P., Edirisinghe, J. N., Mundy, M., Chia, N., Noor, E., Beber, M. E., Best, A. A., DeJongh, M., Kimbrel, J. A., D'haeseleer, P., McCorkle, S. R., Bolton, J. R., Pearson, E., Canon, S., Wood-Charlson, E. M., ... Henry, C. S. (2021). The ModelSEED Biochemistry Database for the integration of metabolic annotations and the reconstruction, comparison and analysis of metabolic models for plants, fungi and microbes. *Nucleic Acids Research*, 49(D1), D575–D588. <https://doi.org/10.1093/nar/gkaa746>

Shreiner, A. B., Kao, J. Y., & Young, V. B. (2015). The gut microbiome in health and in disease. *Current Opinion in Gastroenterology*, 31(1), 69–75. <https://doi.org/10.1097/MOG.0000000000000139>

Steinegger, M., & Söding, J. (2017). MMseqs2 enables sensitive protein sequence searching for the analysis of massive data sets. *Nature Biotechnology*, 35(11), 1026–1028. <https://doi.org/10.1038/nbt.3988>

Sun, Y., Liu, Y., Pan, J., Wang, F., & Li, M. (2019). Perspectives on Cultivation Strategies of Archaea. *Microbial Ecology*. <https://doi.org/10.1007/s00248-019-01422-7>

Thauer, R. K., & Shima, S. (2006). Methane and microbes. *Nature*, 440(7086), 878–879. <https://doi.org/10.1038/440878a>

Varadi, M., Anyango, S., Deshpande, M., Nair, S., Natassia, C., Yordanova, G., Yuan, D., Stroe, O., Wood, G., Laydon, A., Žídek, A., Green, T., Tunyasuvunakool, K., Petersen, S., Jumper, J., Clancy, E., Green, R., Vora, A., Lutfi, M., ... Velankar, S. (2022). AlphaFold Protein Structure Database: massively expanding the structural coverage of protein-sequence space with high-accuracy models. *Nucleic Acids Research*, 50(D1), D439–D444. <https://doi.org/10.1093/nar/gkab1061>

Wang, Z., Zolnik, C. P., Qiu, Y., Usyk, M., Wang, T., Strickler, H. D., Isasi, C. R., Kaplan, R. C., Kurland, I. J., Qi, Q., & Burk, R. D. (2018). Comparison of Fecal Collection Methods for Microbiome and Metabolomics Studies. *Frontiers in Cellular and Infection Microbiology*, 8. <https://doi.org/10.3389/fcimb.2018.00301>

Weinberger, V., Mohammadzadeh, R., Blohs, M., Kalt, K., Mahnert, A., Moser, S., Cecovini, M., Mertelj, P., Zurabishvili, T., Wolf, J., Shinde, T., Madl, T., Habisch, H., Kolb, D., Pernitsch, D., Hingerl, K., Metcalf, W., & Moissl-Eichinger, C. (2024). Expanding the cultivable human archaeome: Methanobrevibacter intestini sp. nov. and strain Methanobrevibacter smithii "GRAZ-2" from human feces. *Under Review*.

Wickham, H. (2016). *ggplot2: Elegant Graphics for Data Analysis*. Springer-Verlag.

Wood, D. E., Lu, J., & Langmead, B. (2019). Improved metagenomic analysis with Kraken 2. *Genome Biology*, 20(1), 1–13.

Zimmermann, J., Kaleta, C., & Waschyna, S. (2021). gapseq: informed prediction of bacterial metabolic pathways and reconstruction of accurate metabolic models. *Genome Biology* 2021 22:1, 22(1), 1–35. <https://doi.org/10.1186/S13059-021-02295-1>

Zinder, S. H., & Salyers, A. A. (2001). Microbial Ecology—New Directions, New Importance. In *Bergey's Manual® of Systematic Bacteriology* (pp. 101–109). Springer New York. https://doi.org/10.1007/978-0-387-21609-6_12